JOURNAL OF THEORETICAL
AND APPLIED MECHANICS
52, 2, pp. 431-442, Warsaw 2014

NUMERICAL SIMULATION AND EXPERIMENTAL BENDING BEHAVIOUR OF MULTI-LAYER SANDWICH STRUCTURES

Jamal Arbaoui
Laboratoire de Physique des Milieux Denses, Metz, France; e-mail: jamal.arbaoui@ensta-bretagne.fr
Yves Schmitt
IUT de Thionville – Yutz, Yutz, France and P.A. Technologies, Thionville, France
J-Luc Pierrot
Laboratoire de Physique des Milieux Denses, Metz, France
François-Xavier Royer
Laboratoire de Physique des Milieux Denses, Metz, France and IUT de Thionville – Yutz, Yutz, France

In this paper, an experimental investigation, an analytical analysis and a numerical model of a typical four-point bending test on a polypropylene honeycomb multi-layer sandwich panel are proposed. The polypropylene honeycomb core is modelled as a single solid and multi-layer of equivalent material properties. Analytical and numerical (finite element) homogenization approaches are used to compute the effective properties of the single honeycomb core and analytical homogenization of the multi-layer one. The results obtained by numerical simulation (finite element) of four-point bending are compared with the experimental results of a polypropylene honeycomb core/composite facing multi-layer sandwich structures.

Keywords: multi-layer sandwich, polypropylene honeycomb, modelling, bending

1. Introduction

Owing to their merits of a high strength/weight ratio, heat resistance, sound insulation and easy assembly, sandwich structures have been widely used in aerospace, automotive and construction industries (Yu and Cleghorn, 2005; Wang and Yang, 2000; Kim and Hwang, 2000). A typical sandwich panel is composed of three layers, in which two thin sheets (faces) of a stiff and strong material are separated by a thick core of low-density materials (Allen, 1961). Considering the very varied use of these materials in numerous fields, it is essential to know their mechanical properties in order to predict and calculate their behaviour in specific and diverse environments. One thus finds the faces possessing particular mechanical characteristics and the honeycomb core being able to have different specific mechanical properties. The assembly of these two parts is carried out by joining, welding or brazing with another material of different behaviour.

The aim of this work concerning the research subject "Modelling of Composite Multi-layer Sandwichs" is to model the bending behaviour of sandwich structures. The main steps in this study are: i) the determination of elastic constants of the material by analytical and numerical homogenization, and ii) the comparison of the results obtained by numerical modelling with the experimental data recorded for a polypropylene honeycomb core/composite facing multi-layer sandwich structure.

2. Sandwich material

2.1. Mechanical properties

A typical sandwich panel consists of two thin faces with a thickness t, separated by a lightweight core of thickness h_c, as illustrated in Fig. 1. The overall depth and width of the panel are h and b, respectively. The faces are typically bonded to the core to provide a load transfer mechanism between the main components of the sandwich panel.

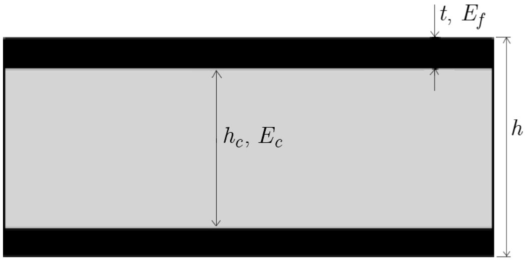

Fig. 1. A structure of a sandwich composite

The flexural rigidity D of a sandwich beam is the sum of flexural rigidities of the faces and the core measured with respect to the centroidal axis of the entire section. It can be expressed as

$$D = \frac{E_f bt^3}{6} + \frac{E_f btd^2}{2} + \frac{E_c bh_c^3}{12} = 2D_f + D_0 + D_c \tag{2.1}$$

where E_f and E_c are Young's moduli of the face sheet and core, respectively, and $d = t + h_c$. D_f is the bending stiffness of the face sheet about its own neutral axis, D_0 – stiffness of the face sheets associated with bending about the neutral axis of the entire sandwich, and D_c – stiffness of the core (Allen, 1961). Since the core is stiff in shear but generally soft, its Young's modulus is much smaller than that of the face sheet. By assuming $E_c \ll E_f$ and the face sheets are thin, the expression for D becomes

$$D \approx E_f \frac{b(h^3 - h_c^3)}{12} \tag{2.2}$$

The shear stiffness Q is given by the following equation

$$Q = G_c \frac{b(h-t)^2}{h_c} \tag{2.3}$$

The face stress is defined such that

$$\sigma_f = \frac{P(L_2 - L_1)}{2tbd} \tag{2.4}$$

In the core, the shear stress is given as

$$\tau_c = \frac{P}{2bd} \tag{2.5}$$

The elastic deflection w_t for a sandwich beam at loading points $(L_2 - L_1)/2$ is the sum of the flexural and shear deflections for a four-point bending (Fig. 2)

$$w_t = w_1 + w_2 = \frac{P(L_2 - L_1)^2(L_2 + 2L_1)}{24D} + \frac{P(L_2 - L_1)}{2S} \tag{2.6}$$

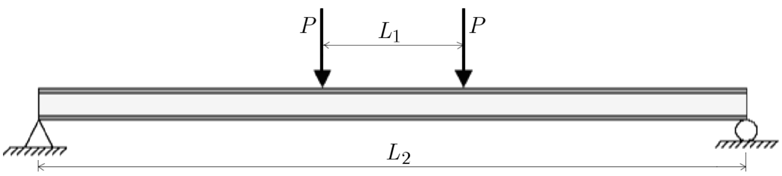

Fig. 2. The four-point bending test

3. Materials and experimental method

3.1. Materials

The sandwich panels used in this study consist of three main parts (Fig. 3):

- Two face sheets of composite glass fibres (T800/M300)/polyester resin with the nominal face thickness of 1 mm
- A honeycomb polypropylene core
- Intermediate layers of composite glass fibres M450/polyster resin with the nominal intermediate layers thickness of 0.05 mm.

The composite structures are pressed in only one pass. The mechanical properties of the basic materials are given in Tables 1 and 2.

Table 1. Mechanical properties of a polypropylene honeycomb core

Properties	Polypropylene honeycomb core
Density [kg/m^3]	80
Shear modulus [MPa]	8
Shear strength [MPa]	0.5
Elastic modulus [MPa]	15

Table 2. Mechanical properties of polyester resin/glass fibres T800/M300 and M450 composites

Properties	T800/M300 composite	M450 composite
Young's modulus [MPa]	9162	5500
Tensile strength [MPa]	321	200
Shear modulus [MPa]	2101	2115
Thickness [mm]	1	0.05
Poisson's ratio	0.3	0.3

3.2. Experimental method

The tests were carried out using a four-point bending testing fixture device shown in Fig. 4. The device, especially designed for such tests, was connected to a servo-hydraulic universal testing machine INSTRON 4302 controlled by an INSTRON electronic unit. These tests were performed with respect to the NFT54-606 norm. To check the reproducibility of the results, five beams by composite type were tested. The crosshead displacement rate was 3 mm/min. The sample dimensions are grouped in Table 3.

Table 3. Specimen dimensions

Specimen	b [mm]	h [mm]	h_c [mm]	L_1 [mm]	L_2 [mm]	L [mm]
Single core	35	22	20	120	300	440
Double core	35	22.05	20.05	120	300	440
Triple core	35	22.1	20.1	120	300	440
Quadruple core	35	22.15	20.15	120	300	440

Fig. 3. Honeycomb multi-layer sandwich

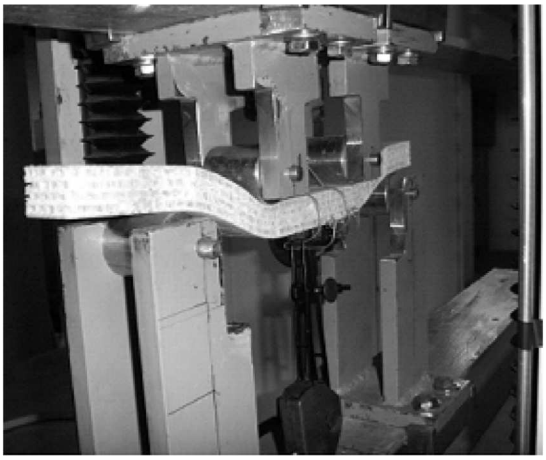

Fig. 4. Static four-point bending test

4. Experimental results

Figure 5 depicts the load-displacement curve for multi-layer honeycomb composite structures solicited in four point bending. The bending behaviour is similar and can be described in three principal phases: the first phase is initial linear elastic behaviour followed by a phase of nonlinear one in which the maximum loading is reached. In the last phase, a reduction in the load applied is observed till the total rupture of the samples. The linear behaviour corresponds to the work of the skins in traction and compression, whereas the nonlinear behaviour mainly depends on the core properties under the effect of the shear stress. This figure shows also an increase of the mechanical properties of facing stress, core shear stress and bending stiffness by about 50, 51 and 36 percent, respectively, as the number of layers increases from single to quadruple layers. The assessed mechanical properties of these composite multi-layers sandwiches are given in Table 4.

Table 4. Mechanical properties of the multilayer sandwich structures

Specimen	Load [N]	Facing stress [MPa]	Core shear stress [MPa]	Bending stiffness [N·mm^2]
Single core	520	63	0.36	$706 \cdot 10^5$
Double core	736	90	0.50	$711 \cdot 10^5$
Triple core	931	113	0.63	$714 \cdot 10^5$
Quadruple core	1065	129	0.72	$718 \cdot 10^5$

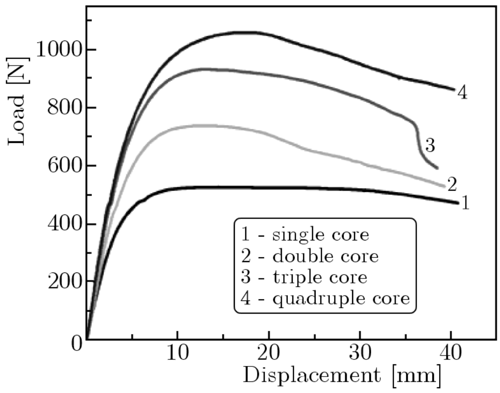

Fig. 5. Typical load/displacement curves for multilayer sandwiches

5. Effective properties of the single honeycomb core

5.1. Analytical homogenization approach

The development of constitutive material models for honeycomb materials is complicated due to highly anisotropic properties of the material. Computationally efficient modelling methods and constitutive laws are required to reduce time and whilst being accurate enough to realistically represent the overall structural behaviour. The analytical expressions used to determine the effective elastic properties of the cellular hexagonal honeycomb core are based on the works of Gibson and Asby (1997), Masters and Evans (1996), Grédiac (1993), Shi and Tong (1995), Becker (1998), Xu and Qiao (2002), Meraghni *et al.* (1999). Appropriate expressions are given in Appendix A.

The elemental beam theory has been adopted (Fig. 6) for each component inside the unit-cell' to arrive at different expressions for effective properties employing the strain energy concept. The length of the diagonal and vertical struts including the angle as well as their thickness have been kept as variable. The presented analytical approach is simple and computes the effective properties in a fraction of the time that is required for FE analysis with a minimum change in the input file. The proper implementation of this method embedded in large quasi-static or dynamic simulations (where a part of the structure could be modelled with a detailed finite element mesh and the rest could be modelled with a single solid layer of equivalent material properties) would give high computational advantage, which is essential in large-scale modelling and simulation environment.

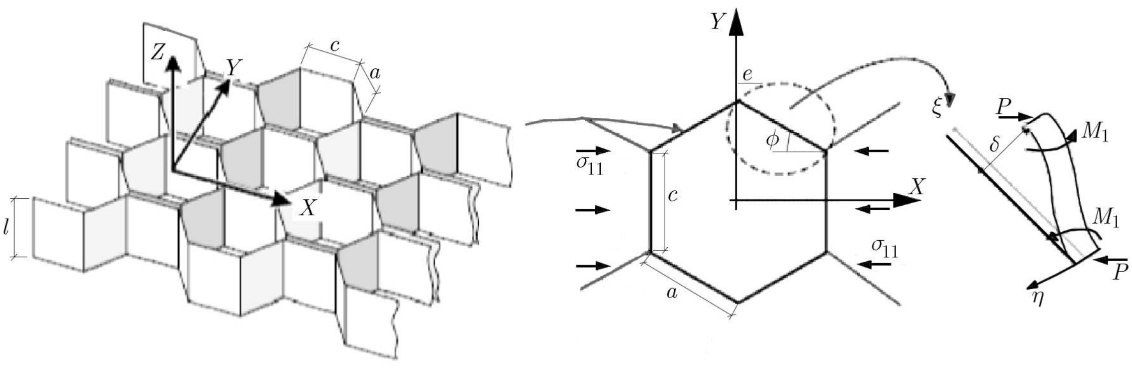

Fig. 6. Deformation mode of a honeycomb structure according to Gibson and Ashby (1997)

5.2. Numerical homogenization approach

The aim is to determine the elastic properties by a numerical homogenization method applied to a Representative Volume Element of the honeycomb to compare the results with those achieved analytically. The Representative Volume Element (RVE) (Fig. 7) consists in 40 cells meshed with plate finite elements with 4 nodes and 6 degrees of freedom per node. Every foil contains 12 elements: 4 according to height and 3 to length. To estimate the various elastic moduli, a displacement is imposed on the face of the RVE in a given direction while the opposite face is being fixed. Symmetries are taken into account by using the appropriate boundary conditions. Nine simulations are necessary to determine nine elastic constants of the single honeycomb. Figure 8 presents an example of the tensile simulation along the direction i $(i = x, y, z)$ which is used to determine the three elasticity moduli E_1, E_2 and E_3 and then six Poisson's ratios. The finite element results are depicted in Table 5.

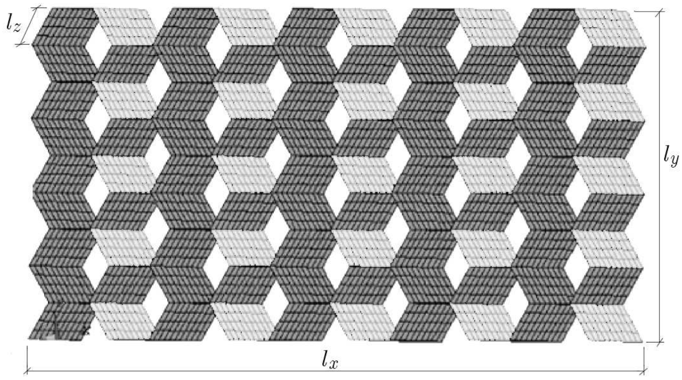

Fig. 7. Representative Volume Element "RVE

In Fig. 7 l_x, l_y and l_z are the lengths of the Representative Volume Element, with: $l_x = 64.7$ mm, $l_y = 36$ mm, $l_z = 10$ mm. The mechanical properties of the honeycomb are related to its geometrical characteristics which are (Fig. 6): $c = a = 4.6188$ mm, $e = 0.24$ mm, $l = 10$ mm, $\phi = 30°$.

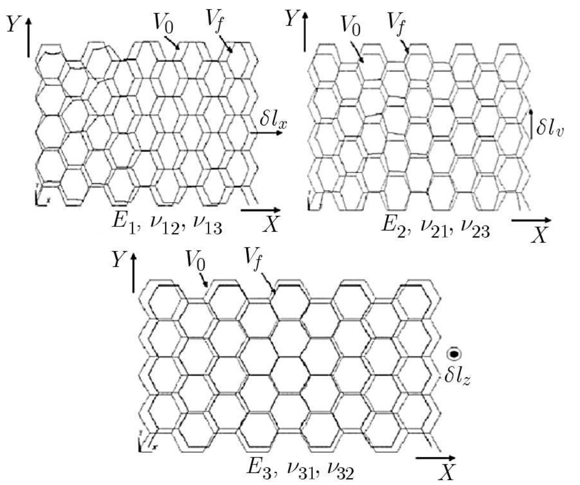

Fig. 8. RVE with the imposed displacement in the X, Y and Z directions

The comparison between the results of Gibson's analytical model and those obtained by the numerical simulation made it possible to better determine the values of the elasticity modulus. One can note that the variation of the results between the numerical simulation and the analytical model is approximately 7.8% for E_1 and 5% for Poisson's ratio, which is relatively

Table 5. Mechanical properties of a single polypropylene honeycomb core

Polypropylene honeycomb	Finite element code (Ansys)	Gibson and Ashby (1997)
E_1 [MPa]	0.448	0.486
E_2 [MPa]	0.545	0.486
E_3 [MPa]	96.3	90
ν_{12}	1.05	1
ν_{13}	0.002	0.002
ν_{23}	0.002	0.002
ν_{31}	0.4	0.4
ν_{32}	0.4	0.4
G_{12} [MPa]	0.1292	0.1214
G_{21} [MPa]	0.0664	
G_{23} [MPa]	16.93	16.44
G_{32} [MPa]	1.2698	
G_{13} [MPa]	17.11	
$G_{13\,min}$ [MPa]		24.673
$G_{13\,max}$ [MPa]		27.415
G_{31} [MPa]	1	

acceptable by taking Gibson's model as the reference. In the case of traction in the Y direction, the variation of the results between the two models is approximately 12% and 25% for E_2 and Poisson's ratio, respectively. For displacement in the Z direction, the variation is approximately 7% for E_3. On the other hand, the variation of Poisson's ratio is very weak. Concerning the shear modulus G_{12}, the variation of the results between Ansys and Gibson are approximately 6.4%. This relatively important error weakly affects the modulus, therefore it has little influence on the sandwich mechanical properties. The shear moduli G_{21}, G_{31} and G_{32} are obtained only by the numerical simulation. Gibson does not give comparative values.

6. Effective properties of the multi-layer honeycomb core

The mechanical characteristics of the M450 intermediate layer (isotropic composite material) are presented in Table 2. The analytical expressions used to assess the effective elastic properties of the multi-layer honeycomb core are determined by the following equation

$$X = \frac{1}{h}\sum_{i=1}^{n} X_i h_i \tag{6.1}$$

The mechanical properties of these composite multi-layer sandwiches are listed in Table 6.

7. Effective properties of the composite T800/M300 face

The composites T800/M300 used in this study are made of fibers well-balanced and oriented along two perpendicular directions: one is called the warp and the other the weft direction. For an approximation of the elastic properties of the fabrics, one can consider them to consist of two plies of the unidirectionals crossing at $90°$ angles with each other. One can then use the following notation: n_1 – number of warp yarns per meter, n_2 – number of fill yarns per meter

Table 6. Mechanical characteristics of the multi-layer core

Multilayer cores	Double core	Triple core	Quadruple core
E_1 [MPa]	14.2	27.84	41.42
E_2 [MPa]	14.2	27.84	41.42
E_3 [MPa]	103.49	116.9	130.27
ν_{12}	1	1	1
ν_{13}	0.002	0.003	0.002
ν_{23}	0.002	0.003	0.002
G_{12} [MPa]	5.39	10.64	15.86
G_{23} [MPa]	10.54	26.84	32.02
G_{13} [MPa]	29.81	35	40.16

$$k = \frac{n_1}{n_1 + n_2} = \frac{1}{2}$$

and fiber modulus: $E_{f'} = 73000\,\mathrm{MPa}$, $G_f = 30000\,\mathrm{MPa}$, $\nu_f = 0.25$; resin modolus: $E_m = 4000\,\mathrm{MPa}$, $G_m = 1400\,\mathrm{MPa}$, $\nu_m = 0.4$; fiber volume fraction $V_f = 28\%$.

One can use the following relations to characterize the unidirectional ply:
— modulus of elasticity along the direction of the fiber

$$E_l = E_{f'} V_f + E_m V_m \tag{7.1}$$

— modulus of elasticity in the direction transverse to the fiber

$$E_t = E_m \Big(\frac{1}{1 - V_f + \frac{E_m}{E_f} V_f} \Big) \tag{7.2}$$

— shear modulus

$$G_{lt} = G_m \Big(\frac{1}{1 - V_f + \frac{G_m}{G_{flt}} V_f} \Big) \tag{7.3}$$

— Poisson's ratio

$$\nu_{lt} = \nu_f V_f + \nu_m V_m \tag{7.4}$$

This two plies of the T800/M300 composite can be considered together. The fabric layer is replaced by a single orthotropic one. One can therefore obtain the mechanical characteristics of the T800/M300 which are determined by the formulas presented in Table 7 (Gay, 1997; Berthelot, 1997). Once the honeycomb core and T800/M300 composite are homogenized, the whole sandwich panel is likened to a beam constituting of three elastic layers: orthotropic/orthotropic/orthotropic that will be used in the numerical model described below.

8. Numerical simulation results

Finite element calculations are also performed on CASTEM 2008. The honeycomb sandwich structure is modelled using 3D solid (eight nodes and six DOFs per node) elements (Mindlin, 1997). For symmetry reasons, only a quarter of the sandwich panel (Fig. 9) is considered in the present analysis. The applied boundary conditions are as follows: at the level of the support, the transversal displacement U_z is fixed to zero; at the symmetry level on face 1, the in-plane

Table 7. Three-dimensional elastic properties of composite T800/M300

E_1 [MPa]	$E_1 = kE_l + (1-k)E_t$	9135
E_2 [MPa]	$E_2 = (1-k)E_l + kE_t$	9135
E_3 [MPa]	$E_3 = E_{matrix}$	4000
ν_{12}	$\nu_{12} = \dfrac{\nu_{lt}}{k + (1-k)\dfrac{E_l}{E_t}}$	0.2
ν_{13}	$\nu_{13} = \dfrac{E_t}{2G_{13}} - 1$	0.3
ν_{23}	$\nu_{23} = \nu_{13}$	0.3
G_{12} [MPa]	$G_{12} = G_{lt} = G_m\left(\dfrac{1}{1-V_f+\dfrac{G_m}{G_f}V_f}\right)$	1616
G_{23} [MPa]	$G_{23} = G_m + \dfrac{G_mV_f}{\dfrac{G_m}{G_f-G_m} + \dfrac{K_m+2G_m}{2K_m+2G_m}(1-V_f)}$	1769
G_{13} [MPa]	$G_{13} = G_m + \dfrac{G_mV_f}{\dfrac{G_m}{G_f-G_m} + \dfrac{K_m+2G_m}{2K_m+2G_m}(1-V_f)}$ Avec $K_m = \dfrac{E_m}{2(1-2\nu_m)}$	1769

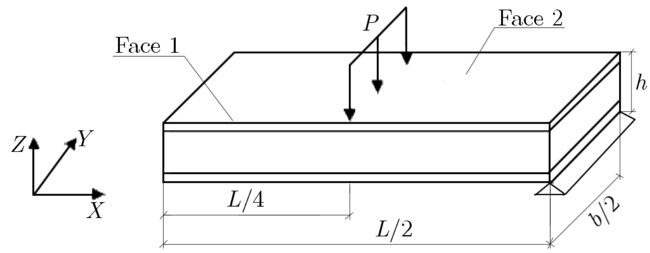

Fig. 9. Modelling of four points on bending CASTEM 2008

displacement U_x and the rotations h_y and h_z are fixed to zero as well; then on face 2, the in-plane displacement U_y and the rotation h_x and h_z are likewise zero.

The sandwich plate is composed of the composite face and multilayer honeycomb core whose dimensions are: length $L = 440$ mm, width $b = 35$ mm, core thickness $h_c = 20$ mm, face thickness $t = 1$ mm and intermediate layer thickness $t' = 0.05$ mm.

Prior to initiating the evaluation study, an analysis of mesh convergence is carried out to ensure the accuracy of the proposed finite element solution since it is considered in the present study as the reference. The convergence was achieved with 4200 elements: 20 elements following the x-axis, 15 elements in the thickness of the core, 3 elements in the thickness of each skin and 10 elements following the y-axis (Fig. 10).

Figures 11a and 11b show the evolution of the load versus the displacement of tow sandwich materials with a single and double core, respectively. These figures compare the bending properties obtained experimentally with that obtained by the 3D finite element model. The values

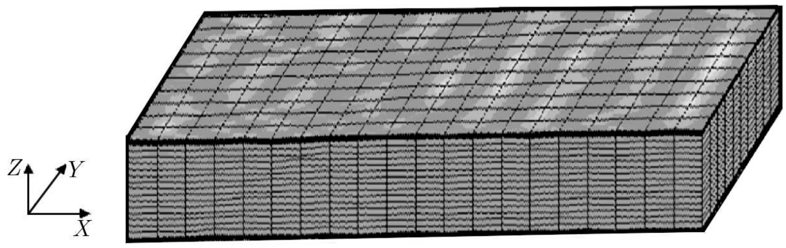

Fig. 10. Finite-element mesh of the sandwich structure

indicate a good prediction of the bending properties with a maximum difference of 7 % between the numerical prediction and experimental results. This gap is very reasonable by taking into account the systematic defects of the manufacturing process, in particular the air bubbles and uncertainties of the used devices.

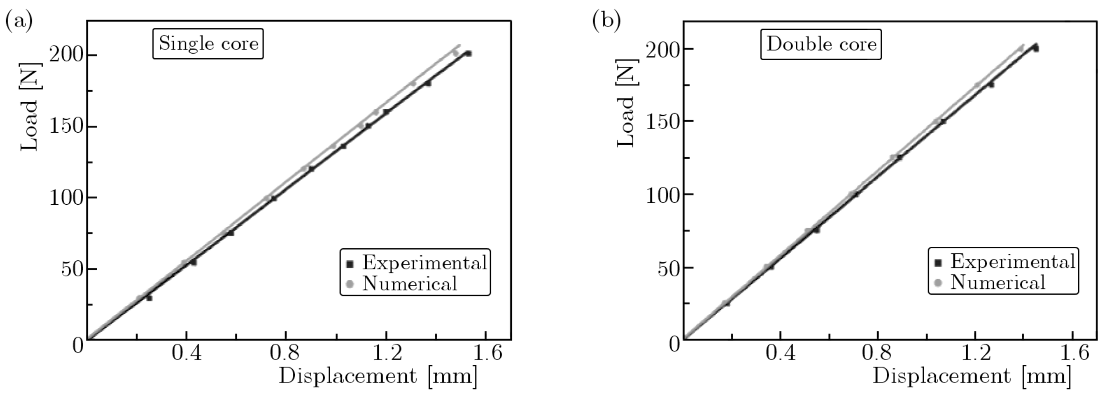

Fig. 11. Comparison of experimental and numerical bending results of the single (a) and double (b) honeycomb

9. Conclusion

Experimental and numerical modelling investigations of a typical four-point bending test of single and multi-layer honeycomb sandwich structures have been performed. Analytical and numerical (FE) homogenization approaches have been used to compute the effective properties of the single and multi-layer honeycomb core as well as the T800/M300 composite face.

The correlation between the effective properties of the single honeycomb core obtained by the analytical and numerical modelling is in good agreement. Compared to the lower bound of Gibson, the shear modulus G13 is low. This can be improved by coupling node cells of the single honeycomb core.

The comparison between the experimental results and those obtained by the numerical simulation of the sandwich structures in honeycomb polypropylene shows a slight difference. This variation remains very reasonable by taking into account the systematic defects of the manufacturing process, in particular the air bubbles and uncertainties of the used devices.

Acknowledgments

The authors would like to gratefully acknowledge P.A. Technologies for instrumenting the polypropylene honeycomb. This work was supported by the Departement de la Recherche et de l'Enseignement Suprieur of REGION LORRAINE, France.

Appendix A

Table 8. The effective elastic properties of honeycomb

Linear elasticity	The effective elastic properties of honeycomb
Tensile modulus in the X_1 direction	$E_1 = E_s\left(\frac{e}{l}\right)^3 \frac{\cos\phi}{(1+\sin\phi)\sin^2\phi}$
Tensile modulus in the X_2 direction	$E_2 = E_s\left(\frac{e}{l}\right)^3 \frac{1+\sin\phi}{\cos^3\phi}$
Shear modulus in the (X_1, X_2) plane	$G_{12} = E_s\left(\frac{e}{l}\right)^3 \frac{1+\sin\phi}{3\cos\phi}$
Poisson's ratio in the (X_1, X_2) plane	$\nu_{21} = \frac{(1+\sin\phi)\sin\phi}{\cos^2\phi}$
Poisson's ratio in the (X_1, X_2) plane	$\nu_{12} = \frac{\cos^2\phi}{(1+\sin\phi)\sin\phi}$
Tensile modulus in the X_3 direction	$E_3 = E_s\left(\frac{e}{l}\right) \frac{\frac{e}{l}+2}{2(1+\sin\phi)\cos\phi}$
Transverse shear	$G_{23} = G_s \frac{1+2\sin^2\theta}{2\cos\phi(1+\sin\phi)} \frac{e}{l}$
Transverse shear	$G_{13} = G_s \frac{\cos\phi}{1+\sin\phi} \frac{e}{l}$
Poisson's ratio	$\nu_{32} = \nu_{31} = \nu$ (solid material)
	$\nu_{13} = \frac{E_1}{E_3}\nu_{31}$ $\quad \nu_{23} = \frac{E_2}{E_3}\nu_{32}$

References

1. Allen H.G., 1961, *Analysis and Design of Structural Sandwich Panels*, Pergamon Press, London, U.K.

2. Becker W., 1998, The in-plane stiffness of honeycomb core including the thickness effect, *Archives of Applied Mechanics*, **68**, 334-341

3. Berthelot J.M., 1996, *Composite Materials: Mechanical Behavior and Structural Analysis* (in French), 4th edition

4. Gay D., 1997, *Composite Materials* (in French), Hermes edition

5. Gibson L.J., Ashby M.F., 1997, *Cellular Solids: Structure and Properties*, 2nd ed., Cambridge University Press, Cambridge, U.K.

6. Grédiac M., 1993, A finite element study of the transverse shear in honeycomb cores, *International Journal of Solids and Structures*, **30**, 13, 1777-1788

7. Kim H.Y., Hwang W., 2002, Effect of debonding on natural frequencies and frequency response functions of honeycomb sandwich beams, *Composite Structures*, **55**, 1, 51-62

8. Masters I.G., Evans K.E., 1996, Models for the elastic deformation of honeycombs, *Composite Structures*, **35**, 403-442

9. Meraghni F., Desrumaux F., Benzeggagh M.L., 1999, Mechanical behaviour of cellular core for structural sandwich panels, *Composites: Part A*, **30**, 767-779

10. Mindlin R.D., 1997, Influence of rotatory inertia and shear in flexural motions of elastic plates, *Journal of Applied Mechanics*, **18**, 31-38

11. Shi G., Tong P., 1995, Equivalent transverse shear stiffness of honeycomb cores, *International Journal of Solids and Structures*, **32**, 10, 1383-1393

12. Wang B., Yang M., 2000, Damping of honeycomb sandwich beams, *Journal of Materials Processing Technology*, **105**, 1/2, 67-72

13. Xu F.X., Qiao P., 2002, Homogenized elastic properties of honeycomb sandwich with skin effect, *International Journal of Solids and Structures*, **39**, 2153-2188

14. Yu S.D., Cleghorn W.L., 2005, Free flexural vibration analysis of symmetric honeycomb panels, *Journal of Sound and Vibration*, **284**, 1/2, 189-204

Manuscript received June 10, 2013; accepted for print September 6, 2013